



SIMPLIFIED MODELING AND SIMULATION OF RUDDER CONTROL FOR PARAMETRIC ROLLING REDUCTION IN SHIPS

Dumitru DELEANU¹

¹Constanta Maritime University, Faculty of Naval Electro-Mechanics, 104 Mircea cel Batran Street, 900663, Constanta, Romania, e-mail address: dumitrudeleanu@yahoo.com

Abstract: Parametric rolling is a resonance phenomenon affecting the safety and operational performance of ships, especially in head or following seas. This paper investigates the possibility of attenuation of parametric roll oscillations by using rudder-based stabilization. To this goal, the ship is represented as a single-degree of freedom oscillator with nonlinear damping and time-varying nonlinear stiffness, subjected to a proportional-derivative (PD) control applied via the rudder. Numerical simulations are performed to measure the influence of the main model parameters, including control gains, initial conditions, encounter wave frequency, on the ship response in roll. Results demonstrate that PD rudder control are able to reduce substantially roll amplitudes for an extensive range of operating conditions. The findings provide insight into the effectiveness of rudder-based control of ship rolling and can be used as a foundation for future research using more complex ship models.

Key words: parametric roll, rudder-based control.

1. INTRODUCTION

Parametric rolling is a nonlinear dynamic phenomenon commonly observed in ships navigating in head or following seas. The main reason for its triggering is the periodic variation of the ship's restoring moment and the result of its development consists in the appearance of excessive roll oscillations that can compromise crew safety and cargo integrity, especially if the wave encounter frequency is twice the ship natural frequency in roll and the wave and ship lengths are almost equal [1, 2].

Over the years, several techniques have been proposed to attenuate it. Passive systems, such as bilge keels or anti-roll tanks, provide limited effectiveness against high-frequency or parametric excitations. Active systems, including fin stabilizers and rudder-based roll stabilization, offer a more adaptable solution to varying sea conditions in real time [3 - 6].

The present study focuses on rudder roll stabilization (RRS), where the ship's rudder is used to generate a corrective roll torque [7, 8]. To this aim, the ship is modelled as a single-degree-of-freedom roll oscillator with nonlinear time-varying stiffness and damping and a proportional-derivative (PD) control is applied through the rudder to counteract roll oscillations.

The rest of the paper is organized as follows: Section 2 describes the mathematical model of the ship in rolling and the rudder-based control system. Section 3 presents the numerical results and the associated

comments. Section 4 concludes with the main findings and highlights the potential directions for further research.

2. MATHEMATICAL MODELING

The governing equation used in the paper for describing the parametric roll oscillation of a ship take account of ship inertia, hydrodynamic nonlinear damping, a time-varying nonlinear restoring moment due to the periodic variation of metacentric height, and the moment generated by the rudder. Thus, it is written as:

$$(I_x + \delta I_x)\ddot{\theta} + d_1\dot{\theta} + d_2|\dot{\theta}|\dot{\theta} + \rho g \nabla (GM_m + GM_a \cos \omega_e t)\theta + k_3\theta^3 = M_{rudder} \quad (1)$$

Here, θ is the roll angle, I_x and δI_x represent the ship and added mass inertia in roll, d_1 and d_2 stand for linear and quadratic roll damping coefficients, ρ is the water density, g the terrestrial gravitational acceleration, ∇ the ship displacement, k_3 the cubic coefficient of the nonlinear restoring moment, GM_m and GM_a are the constant and variable parts of the metacentric height, ω_e represents the wave encounter frequency, and M_{rudder} is the moment generated by the rudder control.

The last quantity is considered to be proportional with the applied rudder deflection δ ,

$$M_{rudder} = k_r \delta \quad (2)$$



where k_r is a constant showing the effectiveness of the rudder in producing an anti-roll torque. The actuation of the rudder is provided by a servomechanism, so the control of the rudder is constrained by the properties of this system. The main constraints are the maximum rudder deflection, δ_{max} , the maximum rate of δ , $\dot{\delta}_{max}$, and the delay, T_δ , between the commanded control input δ_c and the actual angle of the rudder, δ . Usually, these constraints can be incorporated in a first-order differential equation of form:

$$T_\delta \cdot \dot{\delta} + \delta = \delta_c \quad (3)$$

with $|\delta| \leq \delta_{max}$ and $|\dot{\delta}| \leq \dot{\delta}_{max}$.

The rudder-based control is implemented using a proportional-derivative (PD) feedback law of form

$$\delta_c(t) = -(K_p\theta + K_d\dot{\theta})/k_r \quad (4)$$

where K_p and K_d are the proportional and derivative gains. To tune these values, one can use either a manual adjustment or methods as Niegler - Nichols or Cohen-Coon [9].

3. RESULTS AND DISCUSSION

The nonlinear roll model described in the previous section was implemented in MATLAB using *ode45* solver. The running time was set to 400 seconds (with some exceptions) to ensure sufficient observation of the ship response to wave excitation and rudder-based PD control. The ship parameters, taken from experimental research, are presented in Table 1.

Table 1. The parameters involved in Equation (1)

Parameter	Value	Unit
$I_x + \delta I_x$	$1.6184 \cdot 10^{10}$	$kg \cdot m^2$
d_1	$3.2 \cdot 10^8$	$kg \cdot m^2/s$
d_2	$2.99 \cdot 10^8$	$kg \cdot m^2/rad$
k_3	$1.7844 \cdot 10^{10}$	$kg \cdot m^2/s^2 rad^2$
ρ	1000	kg/m^3
g	9.81	m/s^2
∇	76468	m^3
GM_m	1.91	m
GM_a	0.84	m
ω_e	0.592	rad/s

The ship natural frequency in roll is given by:

$$\omega_\theta = \sqrt{\frac{\rho g \nabla GM_m}{I_x + \delta I_x}} = 0.2975 \text{ rad/s}$$

such as $\omega_e/\omega_\theta = 1.99$.

3.1 Single – case dynamics

We first simulated the ship's behaviour in the absence of rudder control. As expected, approaching the resonance condition $\omega_e \approx 2\omega_\theta$ causes any initial disturbance to be greatly amplified. Figure 1 shows the time histories of ship roll angle, $\theta(t)$, the phase plane, $(\theta, \dot{\theta})$, and the ship energy in roll, $E(t) = \frac{1}{2} I_x \dot{\theta}^2 + \frac{1}{2} C_m \theta^2$, where $C_m = \rho g \nabla GM_m$. Even if the ship has good damping, the initial disturbance of 1° , perhaps caused by a gust of wind or a wrong maneuver, is increased in about two minutes to 10° , followed by a slow stabilization to the value of 8.3° . For short time periods this level of rolling generally does not cause permanent damage, but noticeable discomfort for the crew is to be expected and the unsecured equipment may start to shift. A failure of one of the other existing damping systems (possible) would decrease the coefficients d_1 and d_3 values, which would lead to much higher roll angles ($20^\circ - 30^\circ$) and, consequently, to a real danger to the integrity of the cargo and the safety of the crew [10].

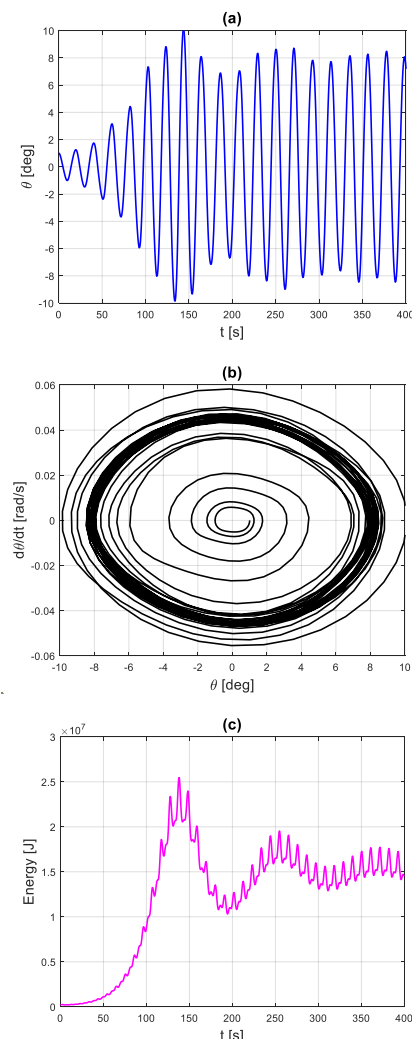


Figure 1 Ship behaviour in the absence of a rudder control: (a) Roll angle time histories; (b) Phase plane; (c) Ship energy.

Then, for cancel out or diminish this undesirable oscillation, the effectiveness of the PD rudder control strategy was evaluated.

The fixed values $k_r = 2 \cdot 10^8 \text{ Nm/rad}$, $T_\delta = 0.5 \text{ s}$, $\delta_{max} = 25^\circ$, $K_d = 10^8 \text{ Nms/rad}$ and variable gain K_p were chosen. Figures 2 and 3 present the roll angle, rudder angle and ship energy for $K_p = 2.5 \cdot 10^8 \text{ Nm/rad}$ and $K_p = 3.0 \cdot 10^8 \text{ Nm/rad}$, respectively.

In first case, the PD controller reduced the roll oscillation to 2.3° . In the second one, we witness to a cancellation of the initial perturbation. The rudder angle δ followed the same trend as the roll angle θ and never exceeded 5° .

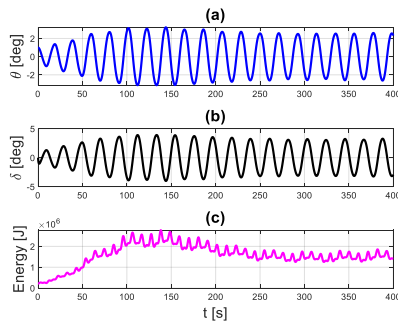


Figure 2 Dependence on time of the roll angle, rudder angle and ship energy for $K_p = 2.5 \cdot 10^8 \text{ Nm/rad}$

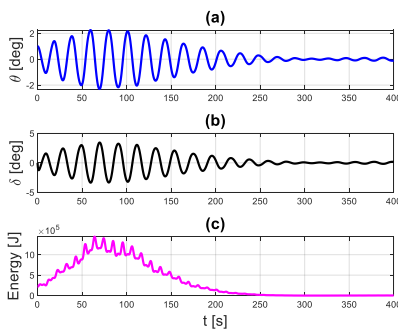


Figure 3 Dependence on time of the roll angle, rudder angle and ship energy for $K_p = 3.0 \cdot 10^8 \text{ Nm/rad}$

3.2 Influence of control gains

To give more insight about the influence of control gains K_p and K_d on the ship rolling, we make use of large-scale of them to generate two dimensional colormaps of maximum rolling and rudder amplitudes, and of final energy of ship rolling (see Figure 4).

For a fixed derivative gain K_d , increasing proportional gain K_p reduces the maximum amplitude of ship rolling in the stationary phase, $\max|\theta|$ and, as

consequence, the ship energy in roll. For a better separation of the plane (K_p, K_d) into areas with slower or faster stabilization of roll oscillations, representative coloured contour lines were used (e.g., $\theta_{max} = 2^\circ$).

The situation is somewhat different in the case of the rudder angle δ . It is possible in some cases that an increase in the parameter K_p will cause the actuator to saturate, i.e., exceed the value δ_{max} . This possibility shows that a careful tuning of PD gains is required to balance roll attenuation and physical limitations of the rudder system.

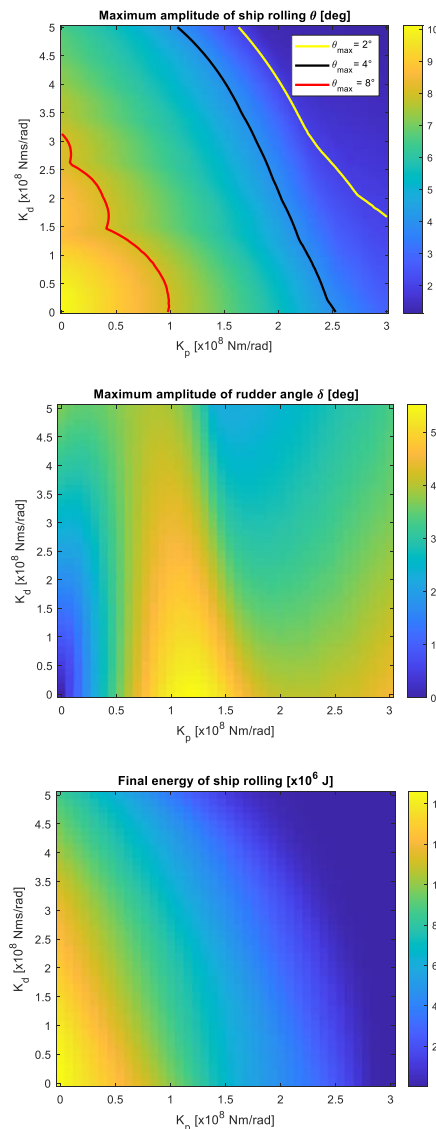


Figure 4 Colormaps for the maximum amplitudes of roll and rudder angles, and the ship's final energy in roll as functions of PD control gains

3.3 Influence of initial conditions

Roll amplitudes and rudder angles are strongly influenced by initial disturbances. With appropriate



control gains, small initial angles $\theta_0 = \theta(0)$ and rates $\dot{\theta}_0 = \dot{\theta}(0)$ result in a rapid ship stabilization and reduced rudder effort. Large disturbances θ_0 and $\dot{\theta}_0$ will maintain the dangerous oscillation for a long period of time, no matter the control gains values.

As Figures 1 and 2 demonstrate, parametric roll develops rapidly in the first 50 - 100 seconds, both in the absence of control and in its presence. In this regard, Figure 5, made with the same inputs as Figure 3, presents colormaps for the dependencies of maximum roll and rudder angles in the first 100 seconds on initial conditions. In the area associated with high θ_0 values, the rudder is seriously stressed and rudder constraint $\delta = \delta_{max}$ is reached.

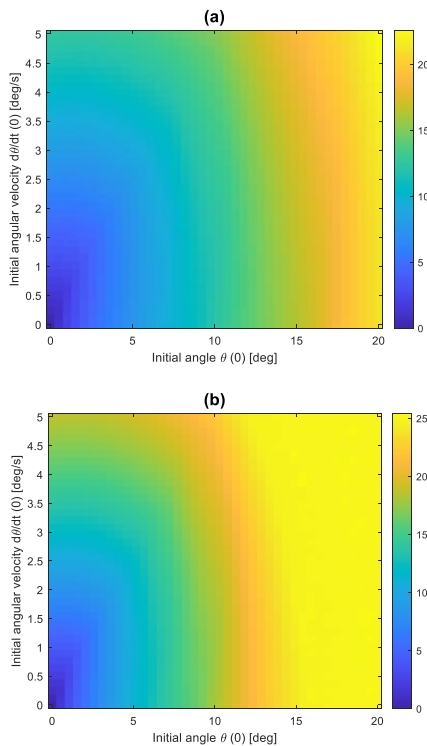


Figure 5 Colormaps for the maximum amplitudes of roll (a) and rudder (b) angles as functions of initial disturbances in the first 100 seconds of simulation

For long term, the robustness of rudder – based PD control succeed to mitigate the roll oscillation. Figure 6 shows the maximum roll angle in the last 50 seconds (from 400) for different $(\theta_0, \dot{\theta}_0)$ and K_p . The other parameters were kept unchanged. A consistent reduction, towards more than acceptable limits, of the roll amplitudes can be observed across the entire range of ICs tested. The most interesting aspect in this simulation is the placement of the roll amplitudes on the strips.

3.4 Roll played by encounter wave frequency

Parametric excitation due to waves can induce resonance, leading to increased roll amplitudes, even in

the presence of a rudder control. Figures 7a and b present angle θ_{max} as a function of wave encounter frequency ω_e for a fixed initial perturbation ($\theta_0 = 1^\circ, \dot{\theta}_0 = 0^\circ/s$) in the first 100 s, respectively last 50 s from 400 s. The results prove that the PD rudder control effectively cancel this small disturbance across the entire frequency range with some exceptions. High amplitudes are observed near the resonance frequency $\omega_e \approx 2\omega_\theta$ even for controlled rudder. For the chosen values of the gain K_p and fixed K_d , only a shifting toward right of the curve $\theta_{max}(\omega_e)$ is observed. This emphasizes the great importance of appropriately tuned control gains to ensure a robust performance under parametric excitation.

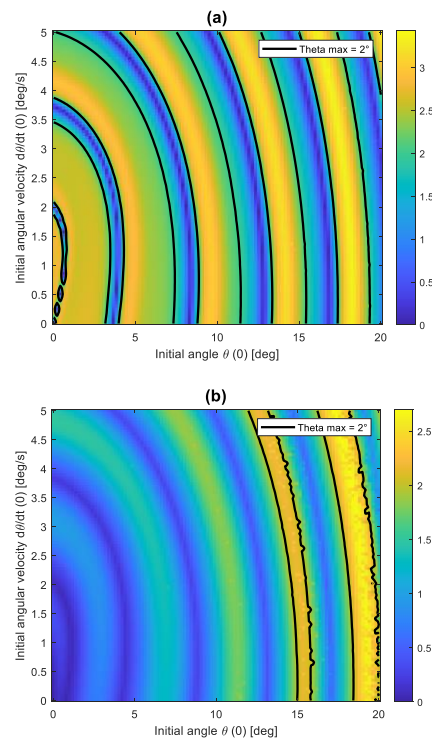


Figure 6 Colormaps for the maximum amplitudes of roll angle as functions of initial disturbances in the last 50 seconds of simulation (from 400).
(a) $K_p = 2.5 \cdot 10^8 \text{ Nm/rad}$;
(b) $K_p = 3.0 \cdot 10^8 \text{ Nm/rad}$

The shift towards higher values of the frequency ω_e with the increase of the gain K_p is illustrated in figure 7c. It is obvious that only a reconsideration of K_p will produce an exit from the area of large stationary amplitudes.

Figure 7b highlights a potentially dangerous frequency range in the case of controlled rudder, located around the value $\omega_e \approx 0.65$. To investigate the control efficiency in this band, Figure 7d shows the angle θ_{max} as a function of the two gains for $\omega_e = 0.67$. In this variant, only values of K_p below 10^8 Nm/rad will ensure a decay of the oscillation.

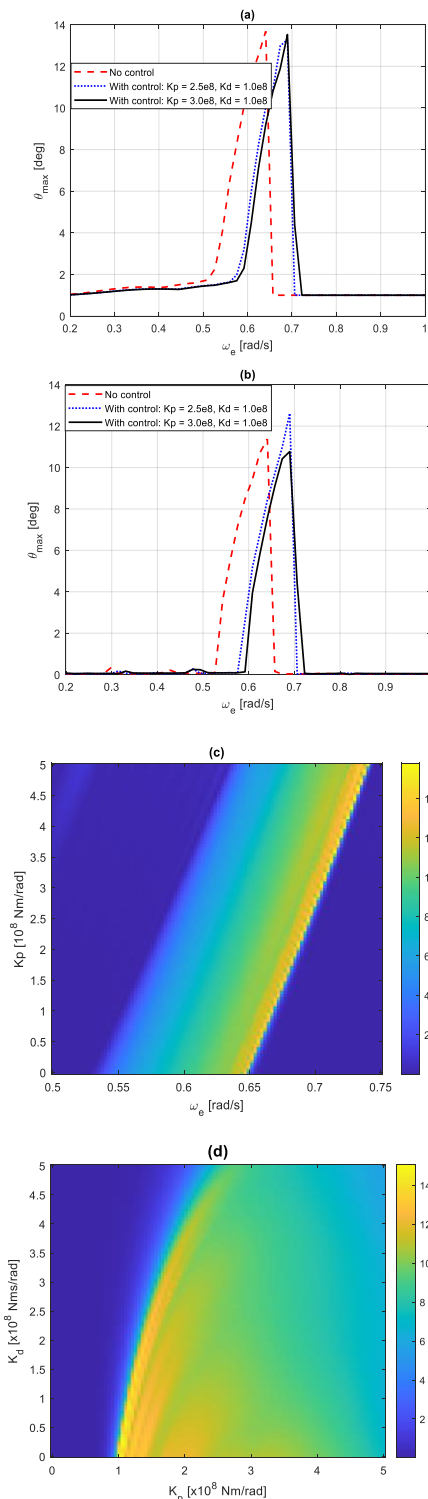


Figure 7 Maximum roll amplitude in the first 100 seconds (a) and in the last 50 s from 400 s (b) as a function of wave encounter frequency; Colormap showing θ_{max} in the last 50 s as a function of ω_e and K_p (c) or K_p and K_d for $\omega_e = 0.67$ (d)

3.5 Influence of an irregular sea



A real wave is generally very different from a sinusoidal one. As a first step towards an irregular wave, we will replace the constant part of the time-varying restoring moment, C_m , by the slowly varying term $C_m(1 + 0.3 \sin 0.05 \pi t)$. The rest of the parameters coincide with those used in creating Figure 6. In addition to a slight increase in the amplitude of the steady state, a deviation from the parallelism of the contour lines is also observed in the right area. It is expected that a stochastic wave model will substantially affect the appearance of these colormaps.

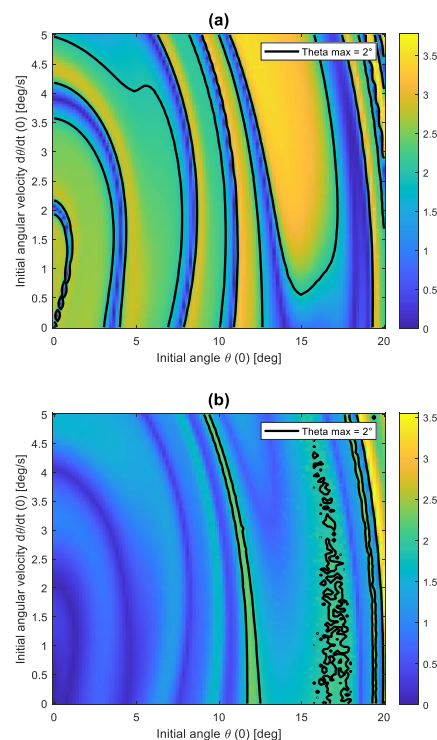
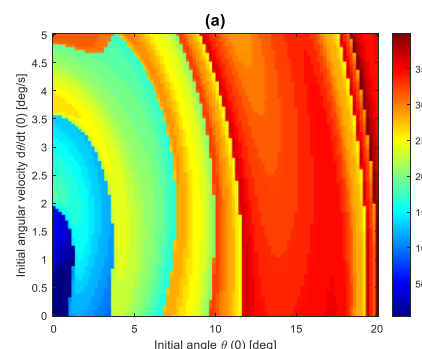


Figure 8 The same as in Figure 6 but for C_m replaced by $C_m(1 + 0.3 \sin 0.05 \pi t)$

3.6 Settling time analysis

In this section, by settling time we understand the time required for $|\theta(t)|$ to remain permanently below a threshold of 1^0 .



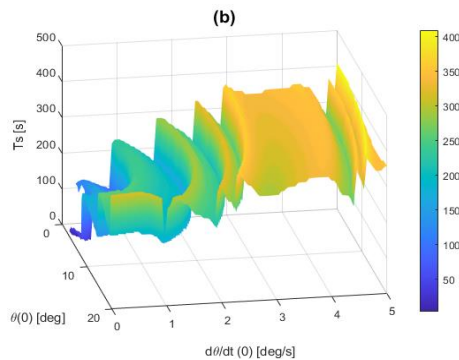


Figure 9 Two (a) and three (b) colormaps describing

4. CONCLUSIONS

The present study investigated the attenuation of parametric roll oscillations in ships using rudder-based proportional-derivative (PD) control. The main findings are summarized as follows:

- i) The PD rudder controller effectively succeeded to diminish or vanish roll amplitudes across a wide range of wave frequencies and initial conditions both in regular or irregular-like seas;
- ii) Roll amplitudes and settling times are strongly dependent on initial perturbations. Small initial roll angles and rates result in a rapid stabilization, while large perturbations cannot be attenuated

5. Credit Author Statement

Conceptualization: D.D.

Data curation: D.D.

Formal analysis: D.D.

Funding acquisition: D.D.

Investigation: D.D.

Methodology: D.D.

Project administration: D.D.

Resources: D.D.

Software: D.D.

Supervision: D.D.

Validation: D.D.

Visualization: D.D.

Writing – original draft: D.D.

the settling time T_S as a function of initial conditions

Figure 9 presents two and three dimensional colormaps of the settling time T_S (in seconds) for different combinations $(\theta_0, \dot{\theta}_0)$ and $\omega_e = 0.592$. The simulation confirms that low initial disturbances lead to short settling times (< 100 s), moderate disturbances result in settling times up to 150 s, while severe initial perturbations require hundreds of seconds for stabilization (if it really happens for the combination chosen for control gains).

regardless the control gains or require long settling times;

- iii) The wave excitation is dangerous only in the proximity of resonance. A suitable choice of control gains will produce a shift of the frequency-response curve and, as consequence, an exit from the high amplitudes region;
- iv) Despite the model's simplifications, the study provides valuable information about rudder-based stabilization of ship rolling.

Future work may include extensions of the model to multi-degree-of-freedom systems, incorporate more nonlinear features and stochastic wave spectra, and/or experiments to validate the numerical predictions.

Writing – review & editing: D.D.

6. REFERENCES

- [1] Ikeda, Y., Ouchi, T., 2008, *Parametric rolling in head seas: Mechanisms and countermeasures*, Journal of Marine Science and Technology, Vol.13, no.2, pp. 123 - 136.
- [2] Pauling, J.R., 2011, *Parametric rolling on ships: then and now. Contemporary ideas on ship stability and capsizing in waves*, Fluid Mechanics and its Applications, Vol. 97, pp. 253 - 266.
- [3] Novac, I., Făitar, C., 2016, *Consideration upon fixed anti-rolling passive systems*, „Mircea cel Batran Naval Academy” Scientific Bulletin, Vol. 19, no. 2, pp. 260 - 266.
- [4] Larsson, L., Stern, F., 2013, *Roll stabilization of ships: A review of active and passive methods*, Journal of Ship Research, Vol. 57, no. 3, pp. 190 - 204.
- [5] Larsson, L., Ory, F., 2017, *Analysis of parametric roll resonance and mitigation using active control systems*, Applied Ocean Research, Vol. 63, pp. 1 - 12.





[6] Liu, B., 2023, *Study of modern ship stabilizer technology*, Highlights in Science, Engineering and Technology, Vol. 72, pp. 788 – 792.

[7] Grue, J., Faltinsen, O.M., 2001, *Rudder-induced roll control in ships under parametric excitation*, Ocean Engineering, Vol. 28, no. 11, pp. 1303 – 1320.

[8] Von Amerengen, J., Van der Klugt, P.G., Van Nauta Lemke, H.R., 1990, *Rudder roll stabilization for ships*, Automatica, Vol. 26, no. 4, pp. 679 – 690.

[9] Tagnacca, S., D'Ambrosio, F., 2015, *PD control of ship roll: Simulation and optimization*, Journal of Marine Science and Application, Vol. 14, no. 2, pp. 102 – 112.

[10] Deleanu, D., Dumitrache, C.L., 2019, *Numerical study of a container ship model for the uncoupled parametric rolling*, IOP Conference Series: Materials Science and Engineering, **591012106**.

